

Supplemental information

Figure legends

Supplementary figure 1. Comparison of emission spectra of CoA-PEG5-NR linked to 2031-ACP-IR in the time-course

Emission spectrum of a representative time-course observation of CoA-PEG5-NR linked to 2031-ACP-IR (Fig. 3C) at time 0 sec, at 230 sec, before insulin treatment, and at 540 sec, the last time point.

Supplementary figure 2. The whole time-lapse image set of Fig. 4 and enlarged image set of ZNCC and Top/Bottom 1000 pixels.

The whole time-lapse image set of GP (a), ZNCC (b) and top/bottom 1000 pixels (c) in Fig.4. Enlarged images of ZNCC time-lapse images (d) and top/bottom 1000 pixels (e).

Supplementary video 1-3.

The time-lapse movies of GP (1), ZNCC (2), and top/bottom 1000 pixels (3). Arrow heads point out the regions often forming membrane ruffling or protrusions.

Supplementary figure 3. Strong laser power induces GP decrease and masks the effect of insulin

Time course of mean delta GP change compared to time 0. After 2 hr serum starvation, cell stably expressing 2031-ACP-IR or transiently were labelled with CoA-PEG5-NR. Spectral imaging was performed using different laser powers and control solution or insulin solution were treated at 120 sec (upper; weaker laser power) or at 180 sec (lower; stronger laser power). Data represent the mean \pm S.E.M of from 10 time-lapse image sets for both control and insulin of stronger laser powers, 11 for control of lower laser power and 13 for insulin of lower laser power.

Supplementary figure 4. Akt phosphorylation is blocked by LY294002 treatment upon insulin stimulation

Akt-phosphorylation upon insulin stimulation in the presence or absence of LY294002. 2031-ACP-IR expressing cells were serum-starved for 2 hr followed by incubation with serum-free medium, medium including 50 μ M of LY294002 or DMSO for 10 min at 37 degrees, then cells were stimulated by 100 nM of insulin at 37 degrees for 5 min and

phosphorylation of Akt was accessed by western blotting analysis using α -Akt antibody (upper bands) and α phospho-Akt antibody (2nd upper bands). Actin was used as a loading control (lower bands).

Supplementary figure 5. Actin cytoskeleton disruption by Latrunculin B

Actin cytoskeleton was disrupted by Latrunculin B treatment. Cells plated on glass-bottom dishes were stained with Sir-Actin at 37 degrees for 1 hr, followed by washing excess Sir-Actin, then cells were treated by DMSO (upper) or 0.2 μ M of Latrunculin B (lower) at 37 degrees for 10 min. Left pictures are Nomarski images and right pictures are images of Sir-Actin.

Supplementary figure 6. Emission spectrum of ACP-GPI

a) Emission spectrum shows the local membrane environment of 2031-ACP-IR is more disordered than that of ACP-GPI. Cells transiently expressing 2031-ACP-IR were stained with CoA-PEG11-NR or NR12S and emission spectrum between 561 and 695 nm was measured from 10 images for CoA-PEG11-NR (n=119 regions of interest (rois)) and from 5 images for NR12S (n=75). Cells transiently expressing wild type ACP-GPI were stained with CoA-PEG11-NR and emission spectrum between 561 and 695 nm was measured from 5 images (n=75). Normalized fluorescent intensities were plotted. b) Our system recognizes the difference in the local membrane environment between wild type ACP-GPI and PGAP2/3 mutant ACP-GPI. Cells transiently expressing wild type ACP-GPI or PGAG2/3 mutant ACP-GPI were stained with CoA-PEG11-NR and emission spectrum between 561 and 695 nm was measured from 6 images (n=35 for wild type and n=36 for PGAP2/3 mutant). c) The emission spectrum of the bulk plasma membrane assessed by NR12S was identical between wild-type ACP GPI expressing cells and PGAP2/3 mutant ACP-GPI expressing cells. The data represents mean \pm S.E.M from 6 images (n=36 rois for each sample).

Methods

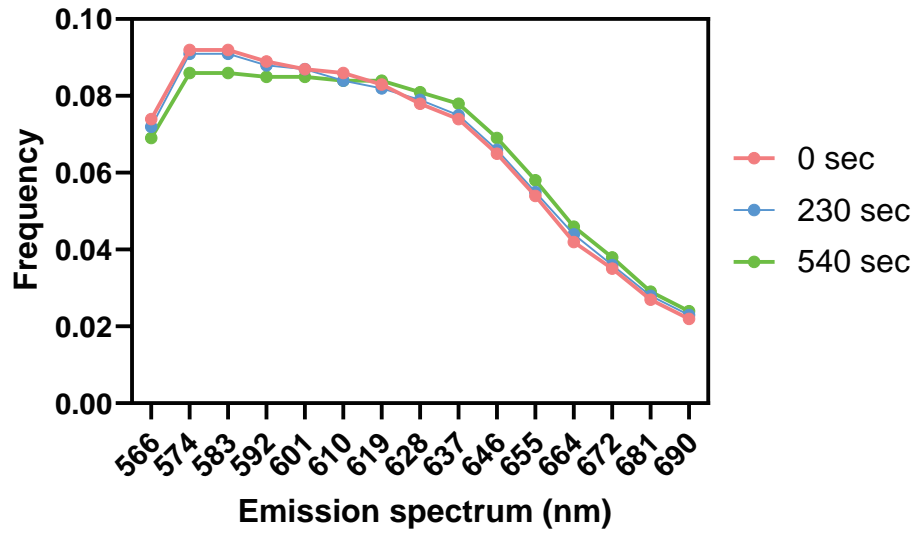
Materials

Anti-Akt mouse monoclonal antibody (Cat. No. 2920) and anti-phospho-Akt rabbit monoclonal antibody (Cat. No. 4060) were purchased from Cell Signaling Tech. Sir-Actin was purchased from Spirochrome and verapamil was purchased from Sigma-Aldrich.

Sir-Actin staining in living cells

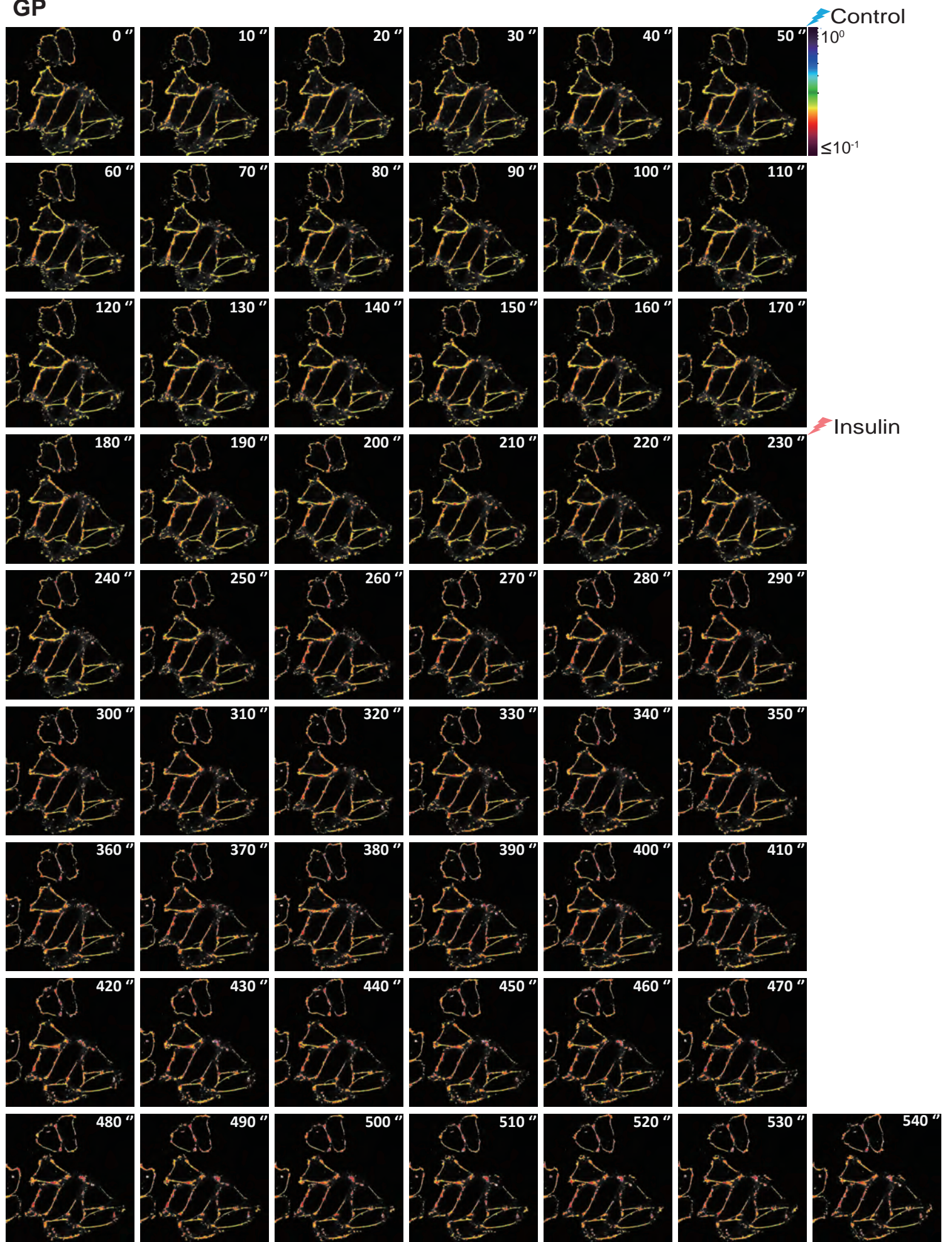
CHO cells stably expressing ACP-2031-IR were incubated with HAM's F-12 HAM medium containing 3 μ M of Sir-Actin and 10 μ M of verapamil at 37 degrees for 1 hr, followed by washing with HAM's F-12 medium 3 times. Imaging of the labelled cells was performed using a Leica SP5 confocal microscope equipped with HCX PL APO CS 63 X oil immersion objective (1.4 NA).

Supplementary figure 1



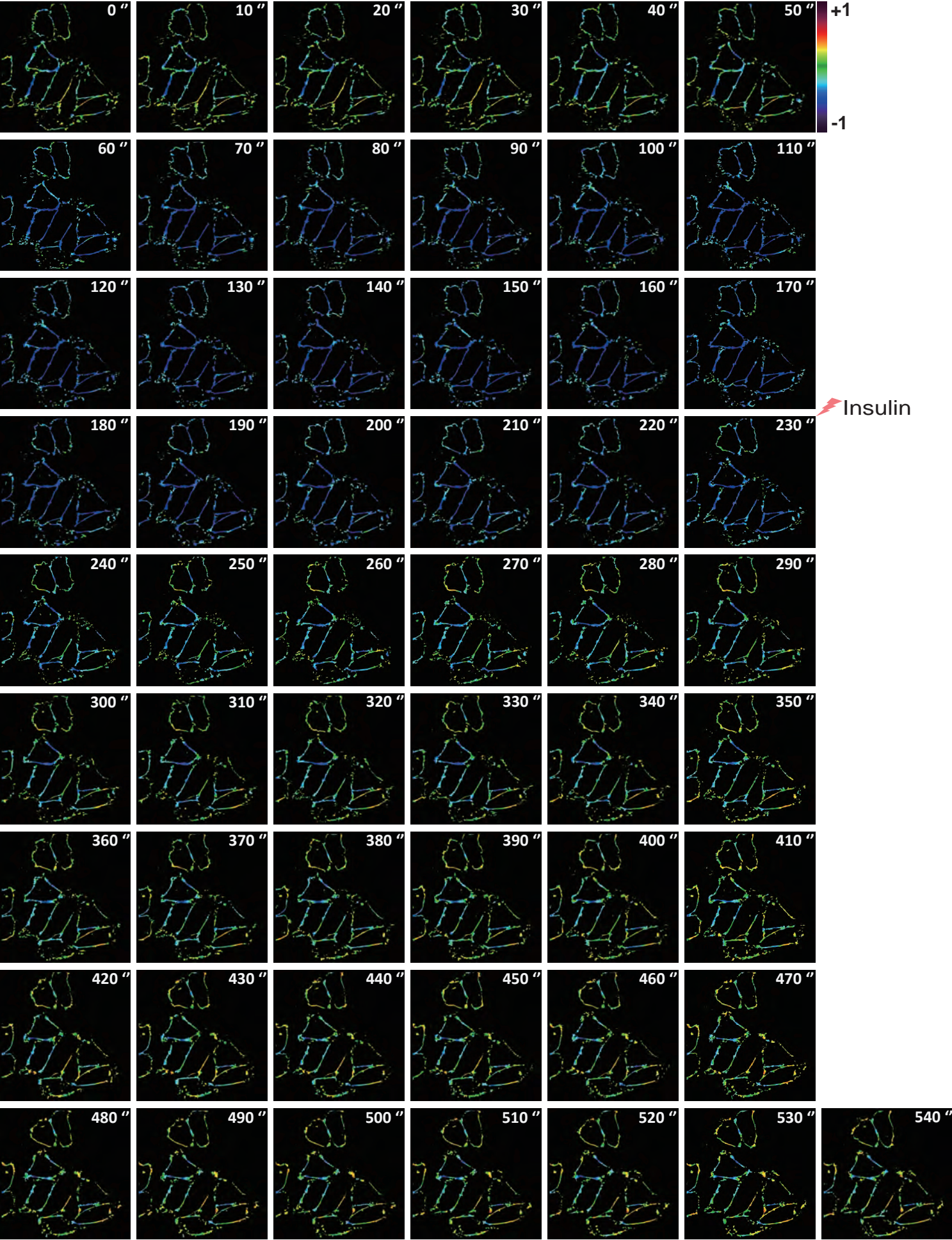
Supplementary figure2 a

GP



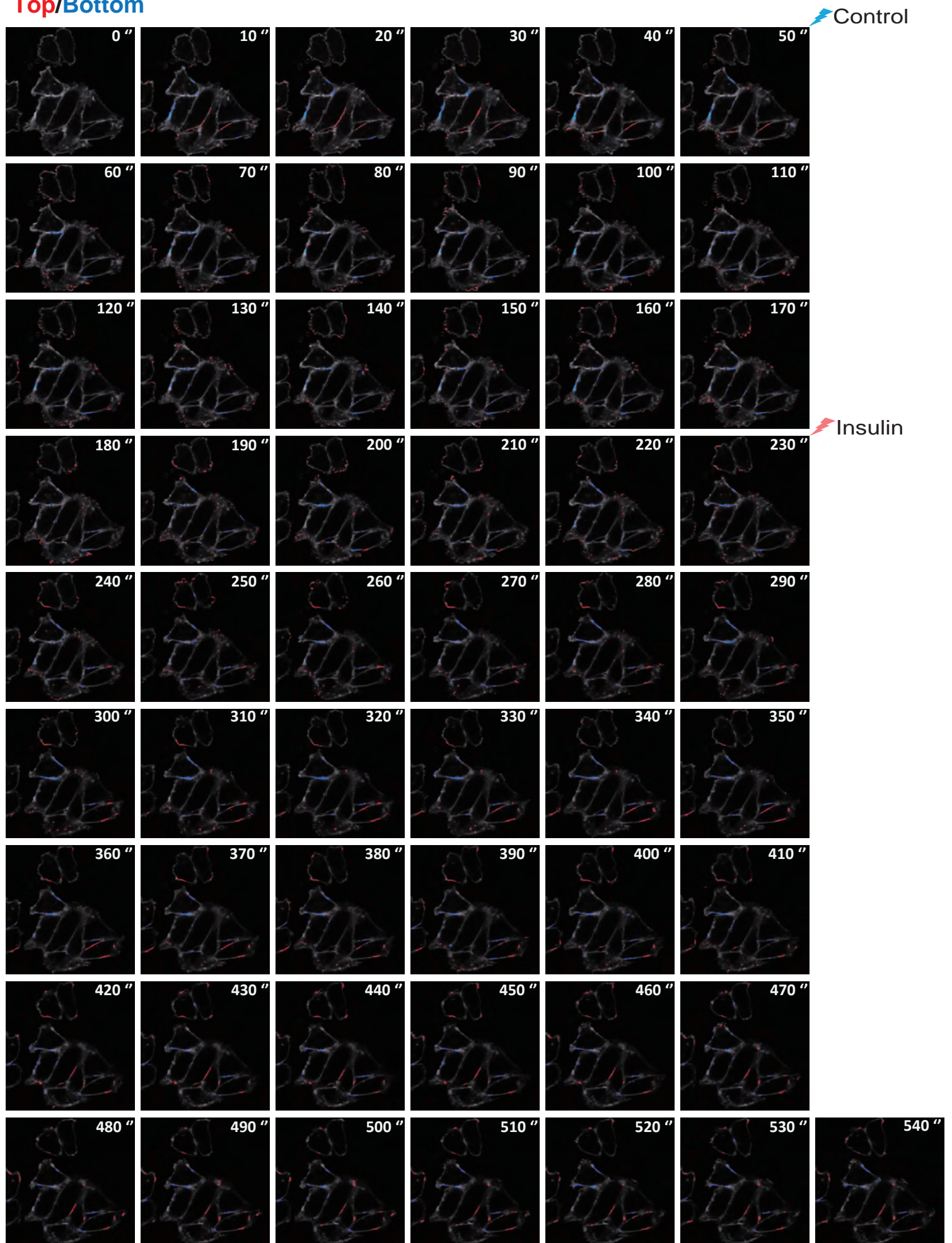
Supplementary figure 2 b

ZNCC



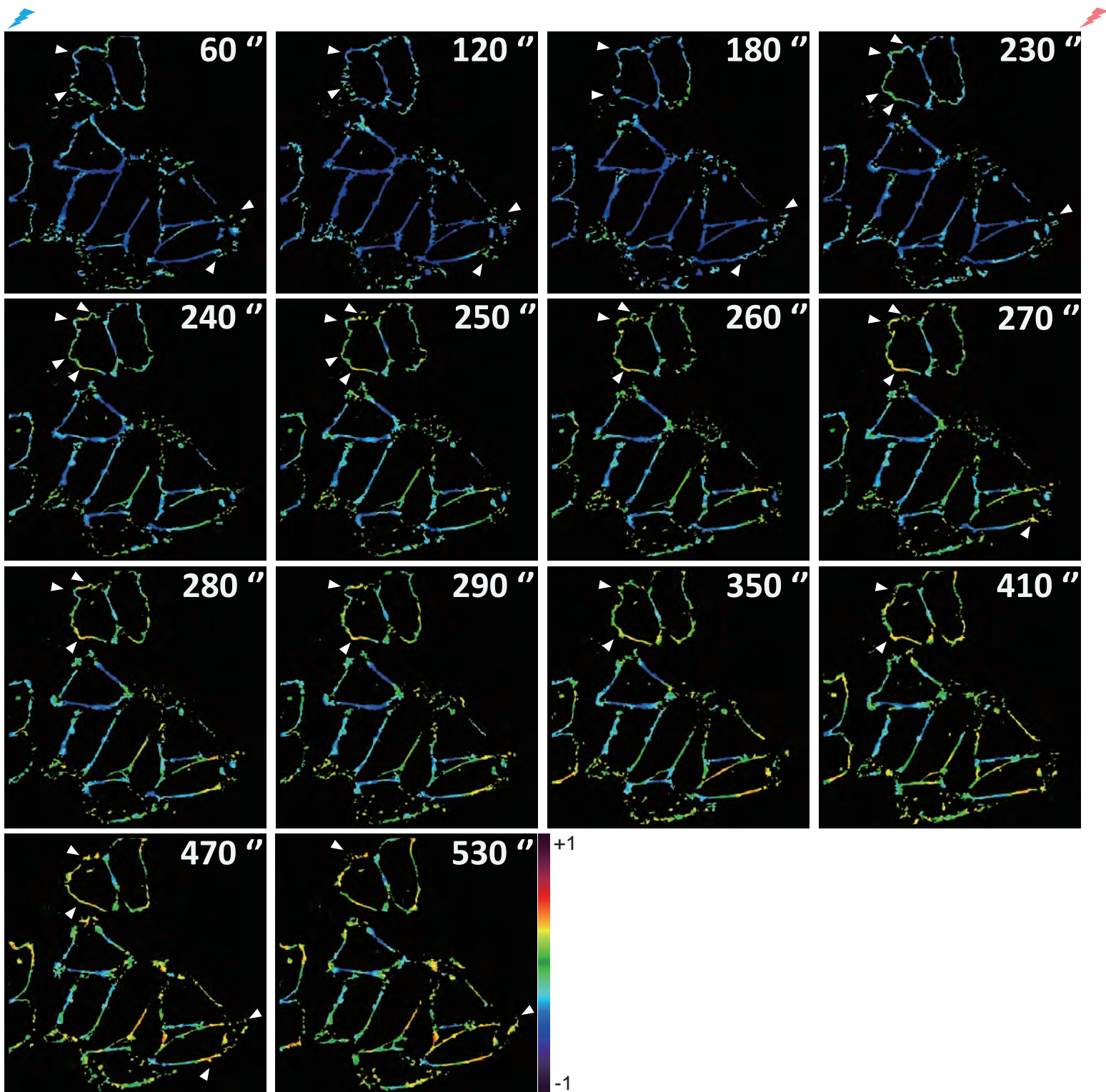
Supplementary figure 2 c

Top/Bottom



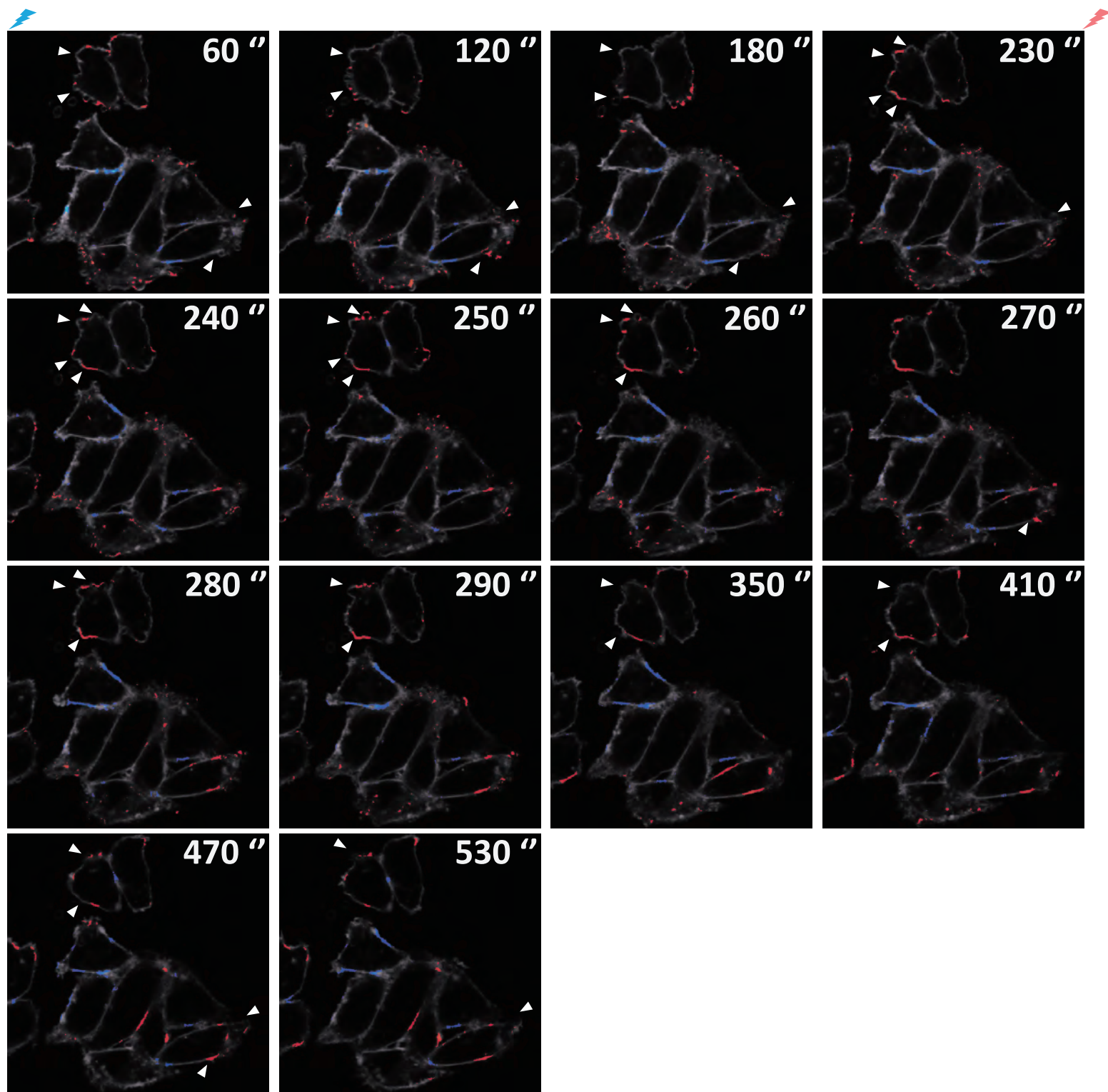
Supplementary figure 2d

ZNCC



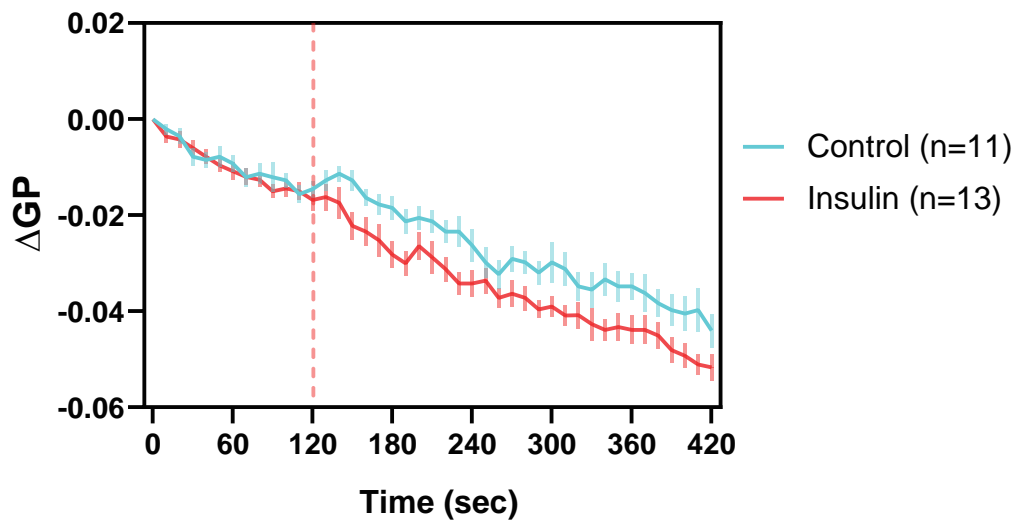
Supplementary figure 2e

Top/Bottom

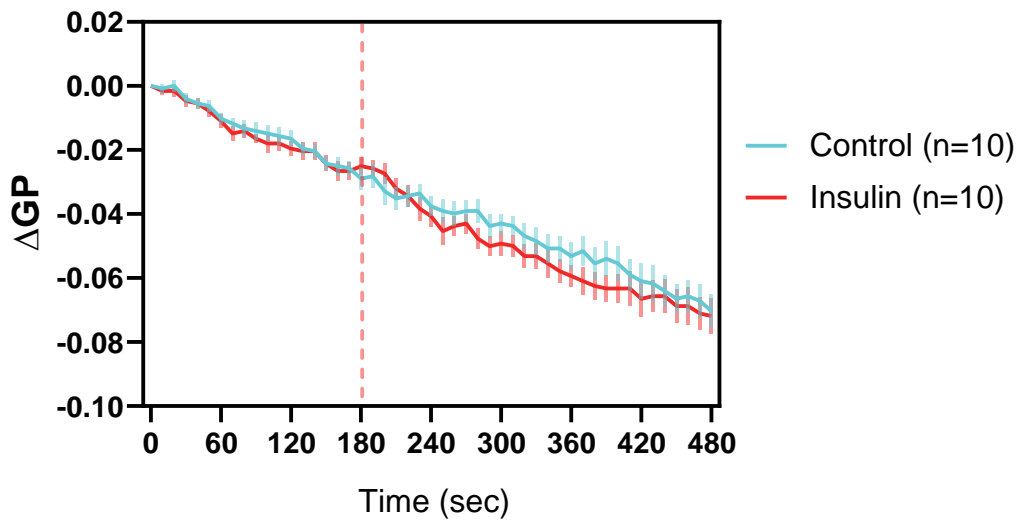


Supplementary figure 3

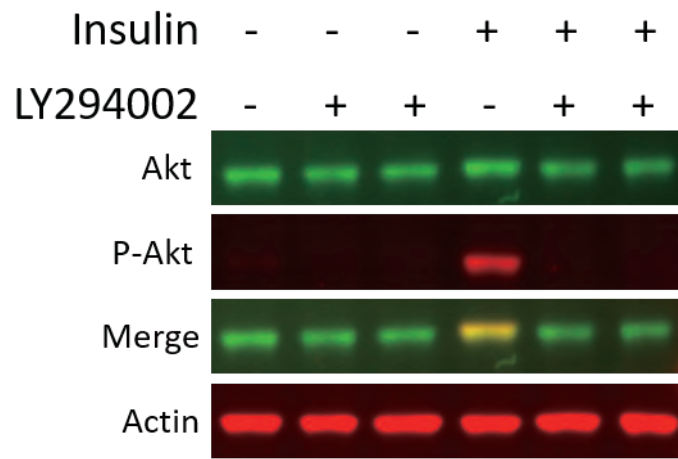
Laser power: 1.8-3%



Laser power: 4-5.5%



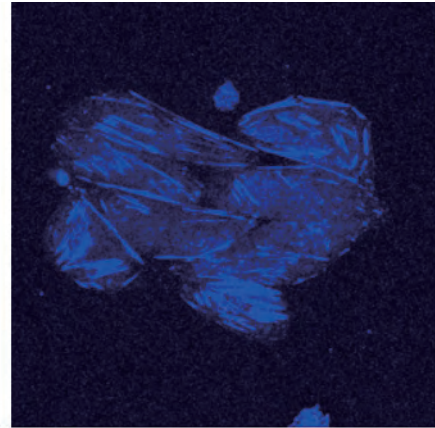
Supplementary figure 4



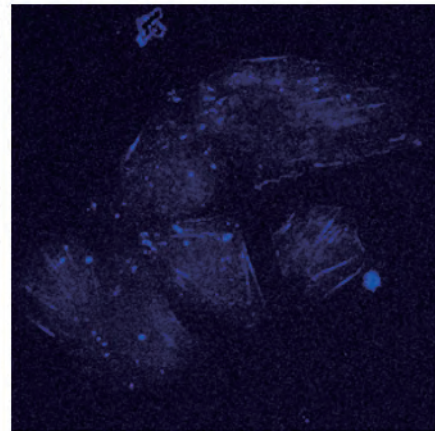
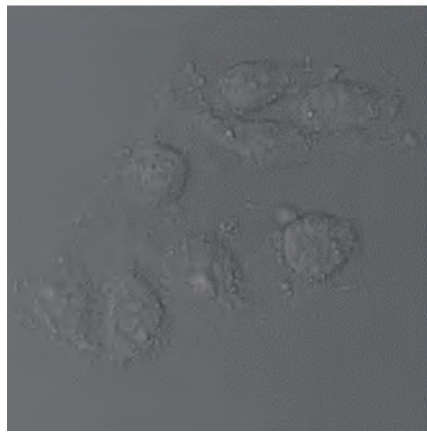
Supplementary figure 5

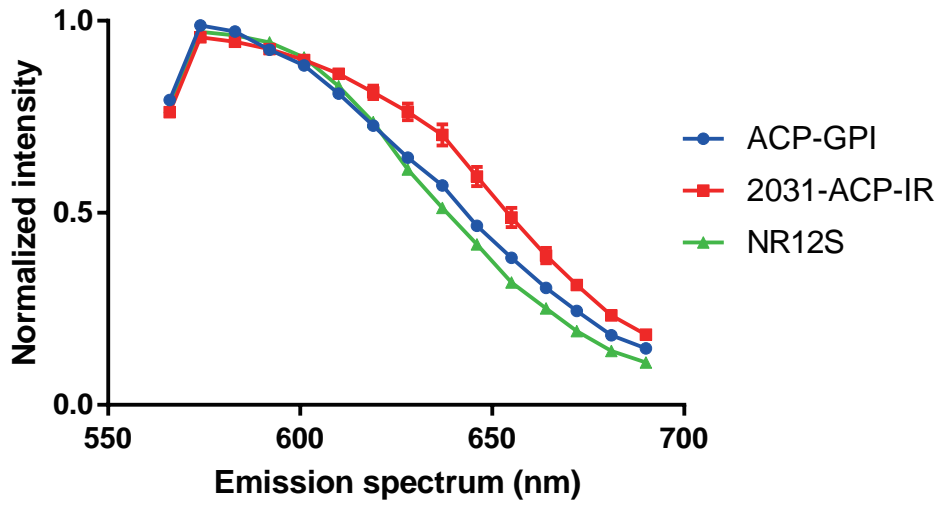
Sir-Actin

Control
(DMSO)

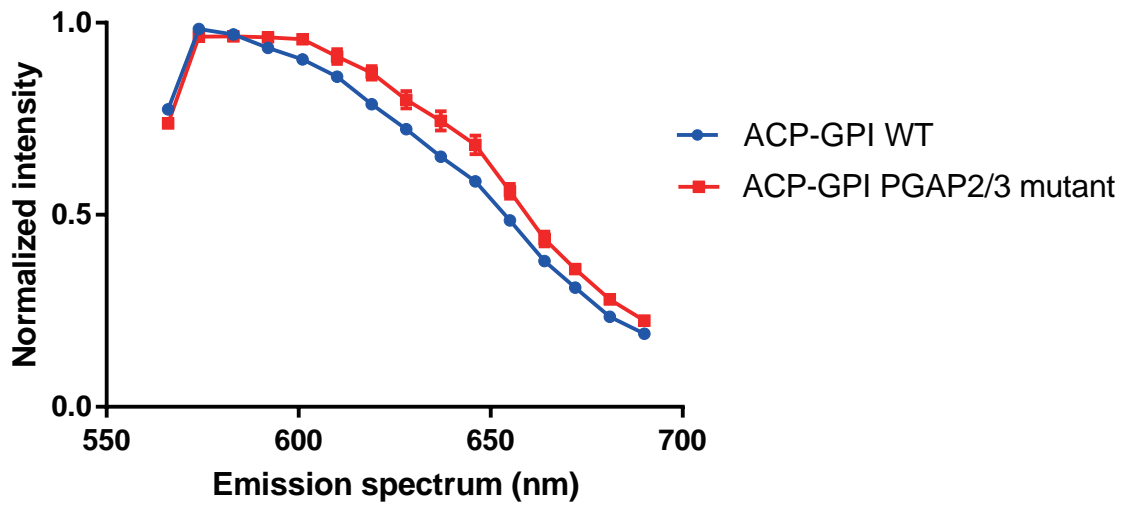


Latrunculin B
(0.2 μ M)

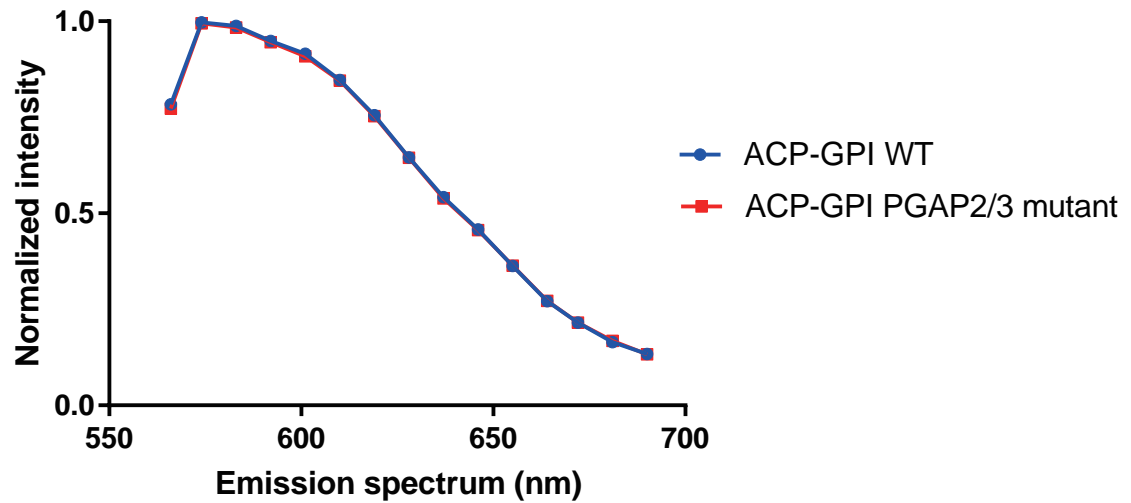




CoA-PEG11-NR



NR12S



Supplementary Information

Supplementary Table 1 | Summary of the primers used in this study.

Plasmid name	Primer	Sequence	Template
Plasmid backbone	pEGFPN1_Gibon F	TCT AGA TCA TAA TCA GCC ATA CCA CAT TTG TAG	pEGFP-N1
Plasmid backbone	pEGFPN1_Gibon R	AAG CTT GAG CTC GAG ATC TGA G	pEGFP-N1
1992-ACP-IR	IR_preACP_F	GAC TCA GAT CTC GAG CTC AAG CTT CCG CCA CCA TGG CCA CCG G	Insulin receptor
1992-ACP-IR	1992-IR_preACP_R	CGA TAG TGC TCA TTT CCG CCT GCC TCT CCC AG	Insulin receptor
1992-ACP-IR	1992-ACP_F	GAG GCA GGC GGA AAT GAG CAC TAT CGA AGA ACG CGT TAA G	ACP
1992-ACP-IR	1992-ACP_R	ACA GCT CAC TGT CCG CCT GGT GGC CGT TGA TG	ACP
1992-ACP-IR	1992-IR_postACP_F	CGG CCA CCA GGC GGA CAG TGA GCT GTT CGA GC	Insulin receptor
1992-ACP-IR	IR_post_R	GTG GTA TGG CTG ATT ATG ATC TAG ATT AGG AAG GAT TGG ACC GAG G	Insulin receptor
2031-ACP-IR	IR_preACP_F	GAC TCA GAT CTC GAG CTC AAG CTT CCG CCA CCA TGG CCA CCG G	Insulin receptor
2031-ACP-IR	2031-IR_preACP_R	CGA TAG TGC TCA TCC CTT TGA GGC AAT AAT CCA GCT CGA ACA G	Insulin receptor
2031-ACP-IR	2031-ACP_F	TTG CCT CAA AGG GAT GAG CAC TAT CGA AGA ACG CGT TAA G	ACP
2031-ACP-IR	2031-ACP_R	AGG GCA GCT TCA GCG CCT GGT GGC CGT TGA TG	ACP
2031-ACP-IR	2031-IR_postACP_F	CGG CCA CCA GGC GCT GAA GCT GCC CTC GAG G	Insulin receptor
2031-ACP-IR	IR_post_R	GTG GTA TGG CTG ATT ATG ATC TAG ATT AGG AAG GAT TGG ACC GAG G	Insulin receptor

PreCT-ACP-IR	IR_preACP_F	GAC TCA GAT CTC GAG CTC AAG CTT CCG CCA CCA TGG CCA CCG G	Insulin receptor
PreCT -ACP-IR	PreCT -IR_preACP_R	CGA TAG TGC TCA TCT TCC TAA ACG AGG ACT CCT CCA GCT C	Insulin receptor
PreCT -ACP-IR	PreCT -ACP_F	CTC GTT TAG GAA GAT GAG CAC TAT CGA AGA ACG CGT TAA G	ACP
PreCT -ACP-IR	PreCT -ACP_R	AAT CCT CAA ACG TCG CCT GGT GGC CGT TGA TG	ACP
PreCT -ACP-IR	PreCT -IR_postACP_F	CGG CCA CCA GGC GAC GTT TGA GGA TTA CCT GCA C	Insulin receptor
PreCT -ACP-IR	IR_post_R	GTG GTA TGG CTG ATT ATG ATC TAG ATT AGG AAG GAT TGG ACC GAG G	Insulin receptor